11. S. S. Friedrich, E. C. Friedrich, L. J. Andrews, R. M. Keefer, *J. Org. Chem.* **34**, 900 (1969); G. A. Russell and K. A. Desmond, *J. Am. Chem. Soc.* **85**, 3139 (1963); G. A. Russell, in *Free Radicals*, J. K. Kochi, Ed. (Wiley, New York, 1973), vol. 1, pp. 275–331.
12. J. F. Blackert and J. M. Tanko, unpublished results.
13. If the rate constant k is not expressed in concentration-independent units such as mole fraction or molality, an additional factor must be included to account for the compressibility of the solvent. For rate constants expressed in units of molarity, the full expression is $[\delta \ln(k)/\delta P]_T = -\Delta V_{act}/RT + \Delta m[\delta \ln(\rho)/\delta P]_T$, where Δm is the difference in the stoichiometric coefficients of the products and reactants and ρ is the solution density. See C. D. Ritchie, *Physical Organic Chemistry, The Fundamental Concepts* (Dekker, New York, ed. 2, 1990), pp. 74–75.
14. T. Asano and W. J. LeNoble, *Chem. Rev.* **78**, 407 (1978).
15. K. Ziegler, A. Späth, E. Schaaf, W. Schumann, E. Winkelmann, *Liebigs Ann. Chem.* **551**, 80 (1942).
16. U. Luning and P S. Skell, *Tetrahedron* **41**, 4289 (1985).
17. Financial support from the U.S. Environmental Protection Agency Office of Pollution Prevention and Toxics, the National Science Foundation (CHEM 9113448), and the Thomas F. Jeffress and Kate Miller Jeffress Memorial Trust Fund is gratefully acknowledged.

13 September 1993; accepted 19 November 1993

Quantum Yield for Production of CH_3NC in the Photolysis of CH_3NCS

Ramón A. Alvarez and C. Bradley Moore*

The ultraviolet spectrum of methyl isothiocyanate (CH_3NCS) and the quantum yield for its dissociation into methyl isocyanide (CH_3NC) and atomic sulfur at 308 nanometers, $\Phi = 0.98 \pm 0.24$, were measured. Methyl isothiocyanate is widely used as an agricultural fumigant and readily enters the atmosphere during and after application. The results indicate that photodissociation by sunlight is an effective pathway for its removal from the atmosphere.

Methyl isothiocyanate (CH_3NCS, MITC) is widely used in agriculture as a soil fumigant; it is a toxic substance that irritates the skin and mucous membranes (*1*). In 1991, 2.1×10^4 metric tons of metam-sodium, which decomposes in the soil to yield MITC,

$$CH_3NHCS_2^-Na^+ \rightarrow CH_3NCS + NaHS$$

were used in the United States (*2*). The California Policy Seminar lists metam-sodium fourth in its priority ranking of high profile pesticides on the basis of 1990 data on applied volumes (*3*). Because of its high vapor pressure (~13 torr at 297 K), MITC can enter the troposphere by spray drift during application or by subsequent volatilization. Estimating that ~60% of the applied dosage of metam-sodium is emitted as MITC into the air (*4*), one finds that $\sim 10^4$ metric tons of MITC were released into the atmosphere in 1991. Concentrations as high as 3 to 242 $\mu g\ m^{-3}$ [1 to 81 parts per billion (ppb)] have been measured at sites downwind from fields injected with metam-sodium (*5, 6*). The threshold for toxicity of MITC is presently under debate; levels above 1 ppb may cause discomfort in some members of the population (*7*).

The persistence of pollutants in the atmosphere may pose health and environmental risks. To assess the potential risks arising from the use of toxic substances, we need to know the dominant mechanism and the rate for their removal from the atmosphere. The fate of species in the troposphere is determined by some combination of (i) photodissociation; (ii) chemical removal, for example, reaction with other trace species such as OH and O_3; and (iii) physical removal, such as through dry deposition or rainout (*8*). This report, which deals with the fundamental photochemistry of MITC, indicates that solar photodissociation could be the chief removal pathway of MITC.

Published ultraviolet (UV) (*9*) absorption spectra of MITC do not cover the spectrum at wavelengths of significant solar flux (wavelengths $\lambda \geq 295$ nm). The NCS radical in various electronic states has been detected as a product of the UV and vacuum-UV photolysis of MITC by a wavelength-selected broadband source (*10*), synchrotron radiation (*11*), and excimer lasers (*12*), as well as from electron impact on MITC (*13*). The photolysis of MITC at 248 and 193 nm also produces small amounts of CN (*12*). The decomposition of MITC in a discharge has been observed to yield NCS (*14, 15*) and CS, CN, and S_2 (*15*). The production of $S(^3P)$ atoms and CH_3NC in solutions of MITC irradiated with 254-nm light has also been reported, with a maximum yield of 45% (*16*). However, nothing is known about the photolysis of MITC at energies corresponding to the long-wavelength tail of its lowest energy absorption band, and the quantum yields of the photolysis products have not been quantified at any wavelength.

The absorption cross section, σ, of MITC is shown in Fig. 1. We focused on the long-wavelength tail that overlaps the spectrum of solar, or actinic, flux (*17*). The absorption band extends out to at least 340 nm, but the wavelength interval from 305 to 330 nm accounts for 86% of the total rate for MITC absorption of the actinic flux in the troposphere. For a photodissociation quantum yield of 1.0, a total absorption rate of $6.7 \times 10^{-6}\ s^{-1}$ yields a lifetime with respect to photolysis of 41 hours for noon sunlight on 1 July at a latitude of 40°N (Table 1). The MITC absorbance was linear in MITC pressure from 1.0 to 9.7 torr. The relative uncertainties in the cross sections at the 95% confidence level were 3, 8, and 23% at 300, 320, and 330 nm, respectively. With a conservative estimate of ±10% for the systematic error in the cross-section determination, the reported values and polynomial fit to the spectrum in Table 1 are believed to be correct to within 10% for $\lambda < 300$ nm, 15 to 20% for $300 \leq \lambda < 320$ nm, and 30% for $320 \leq \lambda \leq 330$ nm. Despite the magnitude of these uncertainties, it is clear that photochemical degradation in the atmosphere could be an effective removal pathway if the photodissociation quantum yield were sufficiently high. We explored this possibility by quantitatively

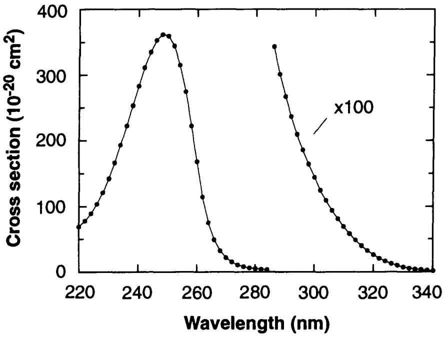

Fig. 1. Ultraviolet spectrum of CH_3NCS. The spectrum was acquired on a Hewlett-Packard 8452 UV/VIS spectrometer with a resolution of 2 nm. The CH_3NCS was pumped at 195 K before use to remove any CS_2 impurity, as verified by mass spectrometry and FTIR spectroscopy (CS_2 concentration ≤ 0.5%). An 8.0-cm quartz cell held the sample, and the evacuated cell served as the blank for all scans. We determined the 100% transmittance level by averaging the percent transmittance values in the 340- to 360-nm range where no signal was detected. All spectra were taken at 298 ± 2 K where $\sigma = A/[P(\text{MITC}) \times (3.25 \times 10^{16}) \times 8.0]$; A is the absorbance (base e), and P is the pressure (in torr).

Department of Chemistry, University of California, and Chemical Sciences Division of the Lawrence Berkeley Laboratory, Berkeley, CA 94720.

*To whom correspondence should be addressed.

studying the yield of photolysis products.

Pure MITC samples (0.7 to 10 torr) were photolyzed with a 308-nm excimer laser. Fourier transform infrared (FTIR) spectroscopy revealed that methyl isocyanide, CH_3NC, was the major stable product formed. The yield of CH_3NC was examined with a diode laser flash kinetic spectrometer (*18*). A diode lasing in the region 2060 to 2190 cm^{-1} with a resolution of 0.0003 cm^{-1} probed the ν_2 band of CH_3NC (*19*). Transient changes in the continuous-wave infrared laser power of 5 parts in 10^4 could be detected, giving a detection limit for CH_3NC of $\sim 5 \times 10^{11}$ molecules per cubic centimeter per shot (signal-to-noise ratio of ~1, in the absence of collisional broadening). All experiments were performed at temperature $T = 298 \pm 2$ K.

The temporal profile of the CH_3NC produced in the 308-nm photolysis of MITC is shown in Fig. 2 (trace a). The CH_3NC production can be described by the combination of direct photolysis and a secondary bimolecular reaction

$$CH_3NCS + h\nu \rightarrow CH_3NC + S(^3P) \quad (1)$$

$$S(^3P) + CH_3NCS \rightarrow CH_3NC + S_2 \quad (2)$$

where h is Planck's constant and ν is the frequency of the 308-nm light. Biexponential fits to the CH_3NC rise show that reactions 1 and 2 each contribute ~50% of the observed signal. We measured the rate constant of reaction 2 to be $(2.0 \pm 0.3) \times 10^{-11}$ cm^3 $molecule^{-1}$ s^{-1} by fitting a single exponential to the slow component of the CH_3NC rise over the MITC pressure range 0.092 to 0.32 torr. The analogous reaction of $S(^3P)$ with HNCS has been observed and proceeds with a rate constant $\geq 3 \times 10^{-11}$ cm^3 $molecule^{-1}$ s^{-1} (*20*).

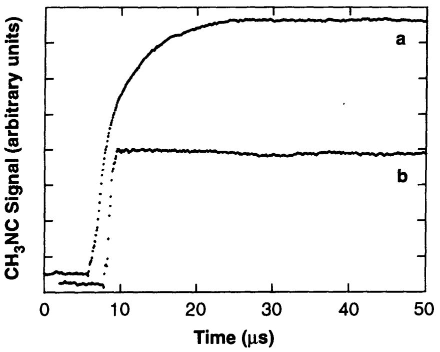

Fig. 2. CH_3NC temporal profiles from the 308-nm excimer laser photolysis of CH_3NCS obtained with a diode laser flash kinetic spectrometer. Conditions: for trace a, 0.300 torr MITC and 3.8 torr SF_6; for trace b, same as for trace a plus 15.9 torr 2-methyl-2-butene. In both traces, the CH_3NC line probed was located at ~2140 cm^{-1} and the UV pulse energy was 32 mJ cm^{-2}. We normalized trace b for the measured collisional broadening by the added 2-methyl-2-butene by multiplying the signal by 2.59. The concentration of CH_3NC from trace b represents 51% of that from trace a, the attenuation resulting from 2-methyl-2-butene scavenging the S atoms produced in reaction 1. Time = 0 μs was arbitrarily offset for clarity.

To determine the photolytic quantum yield for CH_3NC production in reaction 1, we introduced 2-methyl-2-butene, which removed the S atoms by forming a thiirane (*21*)

$$S + CH_3CH{=}C(CH_3)_2 \rightarrow CH_3\overline{CHSC}(CH_3)_2 \quad (3)$$

In the presence of sufficient 2-methyl-2-butene, the CH_3NC signal rises within the ~1-μs time constant of the detector (Fig. 2, trace b). The CH_3NC yield (Table 2) gives $\sigma(308)\Phi = (8.0 \pm 0.6) \times 10^{-21}$ cm^2, the product of $\sigma(308)$, the MITC absorption cross section at 308 nm, and Φ, the quantum yield for dissociation into $CH_3NC + S(^3P)$. The uncertainty is the 95% confidence level for precision. Propagating the estimated uncertainties in the measured quantities that factored into the calculation leads to a total relative uncertainty of 17% (two standard deviations); allowance for systematic error in the experimental method gives $\sigma(308)\Phi = (8.0 \pm 1.6) \times 10^{-21}$ cm^2. Combining $\sigma(308)\Phi$ with $\sigma(308) = (8.1 \pm 1.0) \times 10^{-21}$ cm^2 (Fig. 1) gives $\Phi = 0.98 \pm 0.24$. The measurement of a photodissociation quantum yield near unity is consistent with the lack of structure in the absorption spectrum, which usually suggests a short-lived excited state (*22*).

Because the measured quantum yield applies only at the low total pressures (≤20 torr) used in these experiments, 0.67 torr MITC was photolyzed in 740 ± 20 torr N_2. Analysis of the resulting FTIR spectra for MITC removal and CH_3NC production (with the use of the relative integrated absorptions) revealed that Φ at 740 ± 20 torr is equal to the low-pressure value to within 20%. This suggests that a lower limit for the dissociation rate of excited MITC is 10^{10} s^{-1} and that the MITC UV cross

Table 1. Calculated photolysis rate of MITC. A photodissociation quantum yield of $\Phi = 1.0$ is assumed; the total photolysis rate is $(6.7 \pm 1.7) \times 10^{-6}$ s^{-1}.

Wavelength interval (nm)	Estimated actinic flux* (10^{14} photons cm^{-2} s^{-1})	MITC absorption cross section† (10^{-20} cm^2)	Photolysis rate‡ (10^{-6} s^{-1})
295 to 300	0.031	1.70	0.05
300 to 305	0.335	1.23	0.41
305 to 310	1.25	0.852	1.06
310 to 315	2.87	0.563	1.62
315 to 320	4.02	0.348	1.40
320 to 325	5.08	0.196	1.00
325 to 330	7.34	0.096	0.70
330 to 335	7.79	0.040§	0.31
335 to 340	7.72	0.017§	0.13

*Noon sunlight on 1 July at 40°N latitude; values from (*17*) †The spectra were fit to the polynomial $\sigma = 2.029 - 0.1184\lambda' + 0.002346\lambda'^2 - 1.74 \times 10^{-5}\lambda'^3 + 3.57 \times 10^{-8}\lambda'^4$, where $\lambda' = (\lambda - 294)$ over the interval 294 to 330 nm. ‡Rate = $\Sigma\,[J(\lambda)\sigma(\lambda)\Phi(\lambda)]$, where $J(\lambda)$ is the actinic flux. §Estimated from an MITC spectrum taken at a pressure of 9.7 torr; the uncertainty in these values is estimated to be ±40%.

Table 2. Summary of prompt CH_3NC production in the presence of several different partial pressures *P* of 2-methyl-2-butene (2m2b).

P(MITC) (torr)	*P*(2m2b) (torr)	*P*(CH_3NC)* (mtorr)	Fluence† (10^{16} photons cm^{-2})	$\sigma(308)\Phi$‡ (10^{-21} cm^2)
0.300	15.9§	0.134	5.4	8.3
0.298	5.6§	0.0857	4.0	7.2
0.293	14.2	0.142	6.0	8.0
0.244	16.3	0.133	6.0	9.0
0.128	7.0	0.0586	5.9	7.8
0.220	9.2	0.0858	5.2	7.6
0.263	11.4	0.111	5.4	7.8

*Determined from the magnitude of the transient absorbance and the measured peak absorption coefficient of the probed CH_3NC line, which was normalized for collision broadening. CH_3NC was probed near 2140 and 2158 cm^{-1}. †Measured with a calibrated volume-absorbing disc calorimeter with the rear CaF_2 cell window removed; 6.7% was added for back reflection from the two window surfaces. The index of refraction of CaF_2 at 308 nm is 1.453 (*29*). A 7.0-mm-diameter circular mask was placed before the cell to define the cross-sectional area of the excimer beam ‡$\sigma(308)\Phi = P(CH_3NC)/[P(MITC) \times \text{fluence}]$ §3.8 torr SF_6 was also added as a buffer.

sections and CH$_3$NC quantum yield can be extrapolated with confidence to atmospheric pressure to model the photochemical removal of MITC in the atmosphere. Experiments should be carried out to determine the importance of additional MITC removal pathways, such as reaction with OH, to gain a more complete understanding of its fate.

The persistence, fate, and health consequences of CH$_3$NC should also be examined because it is the principal stable MITC photodegradation product at solar wavelengths. Because CH$_3$NC does not absorb light with $\lambda >$ 260 nm ($\sigma < 10^{-21}$ cm^2) (*23*), it is stable with respect to photolysis in the troposphere. At present, no toxicological data exist for CH$_3$NC; it has an unpleasant odor and is thought to behave like CO in binding to hemeproteins (*24*). The transformation of CH$_3$NC to CH$_3$NCO has been observed in laboratory photolysis studies of MITC in the presence of O$_2$ (*25*) and is adequately described by the photo-oxidation of CH$_3$NC by SO$_2$. Although this mechanism does not apply under atmospheric conditions because SO$_2$ does not build up to sufficiently high levels, the reaction of CH$_3$NC with O$_3$, NO$_x$, or HO$_2$ might result in production of the highly toxic (*26*) CH$_3$NCO. The conversion of alkyl isocyanides to isocyanates by O$_3$ (*27*) and NO (*28*) has been observed in solution. Laboratory studies on the chemistry of CH$_3$NC, along with accurate field measurements of MITC, CH$_3$NC, and CH$_3$NCO concentrations, are thus needed to adequately assess the health risks resulting from the agricultural use of metam-sodium.

REFERENCES AND NOTES

1. Nihon Schering K. K. and Shionogi and Co., Ltd., *J. Pestic. Sci.* **15**, 297 (1990).
2. "Fumigants and nematicides," in *Chemical Economics Handbook* (SRI International, Palo Alto, CA, 1993).
3. J. C. Robinson and W. S. Pease, *California Policy Seminar Brief 5* (1993).
4. M. Leistra and S. J. H. Crum, *Water Air Soil Pollut.* **50**, 109 (1990).
5. F. van den Berg, *Atmos. Environ. Part A* **27**, 63 (1993).
6. "Ambient Air Monitoring in Contra Costa County During March 1993 After an Application of Metam-Sodium to a Field" (California Air Resources Board, Monitoring and Laboratory Division, Sacramento, CA, 1993).
7. M. J. DiBartolomeis *et al.*, "Evaluation of the Health Risks Associated with the Metam Spill in the Upper Sacramento River" (Office of Environmental Health Hazard Assessment, California Environmental Protection Agency, Berkeley, CA, 1992).
8. J. Heicklen, *Atmos. Environ.* **16**, 821 (1982).
9. S.-C. Woo and T. C. Chu, *J. Chin. Chem. Soc.* **5**, 162 (1937); C. N. R. Rao, J. Ramachandran, S. Somasekhara, *Curr. Sci.* **27**, 474 (1958); E. Svatek, R. Zahradnik, A. Kjaer, *Acta Chem. Scand.* **13**, 442 (1959).
10. P. D'Amario, G. DiStefano, M. Lenzi, A. Mele, *J. Chem. Soc. Faraday Trans. 1* **68**, 940 (1972).
11. I. Tokue, A. Hiraya, K. Shobatake, *Chem. Phys.* **117**, 315 (1987).
12. F. J. Northrup and T. J. Sears, *J. Chem. Phys.* **93**, 2337 (1990).
13. I. Tokue, K. Kobayashi, T. Honda, Y. Ito, *J. Phys. Chem.* **94**, 3485 (1990).
14. R. Holland, D. W. G. Style, R. N. Dixon, D. A. Ramsay, *Nature* **182**, 336 (1958).
15. J. E. Nicholas and C. A. Amodio, *J. Chem. Soc. Faraday Trans. 1* **76**, 1669 (1980).
16. U. Schmidt, K. Kabitzke, I. Boie, C. Osterroht, *Chem. Ber.* **98**, 3819 (1965); R. Jahn and U. Schmidt, *Monatsh. Chem.* **109**, 161 (1978).
17. B. J. Finlayson-Pitts and J. N. Pitts, *Atmospheric Chemistry: Fundamentals and Experimental Methods* (Wiley, New York, 1986), p. 134.
18. R. A. Alvarez and C. B. Moore, *J. Phys. Chem.*, in press.
19. H. W. Thompson and R. L. Williams, *Trans. Faraday Soc.* **48**, 502 (1952).
20. C. R. Boxall and J. P. Simons, *J. Photochem.* **1**, 363 (1972–73).
21. O. P. Strausz, in *Sulfur in Organic and Inorganic Chemistry*, A. Senning, Ed. (Dekker, New York, 1972), vol. 2, chap. 11; D. D. Davis and R. B. Klemm, *Int. J. Chem. Kinet.* **5**, 841 (1973).
22. J. G. Calvert and J. N. Pitts, *Photochemistry* (Wiley, New York, 1967), p. 584.
23. B. K. Dunning, D. H. Shaw, H. O. Pritchard, *J. Phys. Chem.* **75**, 580 (1971).
24. H. M. Walborsky and M. P. Periasamy, in *The Chemistry of Functional Groups, Supplement C*, S. Patai and Z. Rappoport, Eds. (Wiley, New York, 1983), p. 836.
25. J. D. Geddes and G. C. Miller, unpublished results; R. A. Alvarez, thesis, University of California at Berkeley (1993).
26. The Occupational Safety and Health Administration's 8-hour Permissible Exposure Level (PEL) is 20 ppb (Sigma/Aldrich Material Safety Data Sheet on CD-ROM, revision 2.14).
27. H. Feuer, H. Rubinstein, A. T. Nielsen, *J. Org. Chem.* **23**, 1107 (1958).
28. T. Saegusa, S. Kobayashi, Y. Ito, *Bull. Chem. Soc. Jpn.* **43**, 275 (1970).
29. D. F. Bezuidenhout, in *Handbook of Optical Constants of Solids*, E. D. Palik, Ed. (Academic Press, San Diego, CA, 1991), p. 831.
30. The authors thank G. C. Miller for pointing out that CH$_3$NCO could be formed in this system. This work was supported by the Director, Office of Energy Research, Office of Basic Energy Sciences, Chemical Sciences Division of the U.S. Department of Energy, under contract DE-AC03-76SF0098.

19 August 1993; accepted 16 November 1993

Structure of Solidified Colloidal Array Laser Filters Studied by Cryogenic Transmission Electron Microscopy

Eduardo A. Kamenetzky,* Lino G. Magliocco, Hans P. Panzer

Ordered arrays of charged uniform colloidal polystyrene particles in solution form a single-wavelength laser filter that is transparent to other wavelengths. A usable filter was prepared by solidification within an acrylamide–methylene-bisacrylamide gel. The rejection wavelength of the colloidal array filter changes with gel composition. Cryogenic transmission electron microscopy of two gel formulations shows that the colloidal array filter is composed of AAA stacking of close-packed planes. Excellent agreement is found between the layer spacings measured and those predicted from the rejection wavelengths.

Suspensions of highly charged colloidal particles (polyballs) or macromolecules form crystalline arrays at particular regions of a ternary phase diagram whose locations depend on particle concentration, counterion concentration, and temperature (*1, 2*). Many naturally occurring colloidal crystalline arrays exist, for example, certain viruses, opal crystals, and solutions of macroions, proteins, cells, ionic micelles, and polynucleotides (*3, 4*). Polyball suspensions are a unique model system for understanding the behavior and stability of real colloidal dispersions (*5*). They also constitute a well-understood experimental system that can be used to model three-dimensional (3D) and two-dimensional (2D) phase transitions in quiescent and sheared crystals (*3, 6*). Polyball colloidal crystals can also function as optical wavelength rejection filters (*7*).

However, colloidal array filters (CAF) in aqueous suspensions have very limited temperature and mechanical stability. Freezing destroys CAFs, high temperature causes the crystalline array to melt, and mechanical shock destroys particle ordering. To produce potentially practical filters, we need a way of solidifying a CAF while preserving its optical properties. Recently, an intermediate step toward a solid CAF was demonstrated: solidification of the suspension within a gel (*8*). The structures of these solidified CAFs were studied by cryogenic transmission electron microscopy (CTEM) (*9*).

There are many potential applications for solidified CAFs in the fields of laser medicine, laser spectroscopy, and laser eye protection. Two CAF properties that are of particular interest are their transmittance of <1% at the rejection wavelength and a narrow bandwidth ≈20 nm. It is thus possible to reject a single wavelength while observing the remainder of the visible spectrum. For example, a surgeon could use a laser, spot its precise location, and at the

---

CYTEC Research and Development, 1937 West Main Street, P.O. Box 60, Stamford, CT 06904.

*To whom correspondence should be addressed.